Check for updates

FULL-LENGTH ORIGINAL RESEARCH

Epilepsia®

Quantitative positron emission tomography–guided magnetic resonance imaging postprocessing in magnetic resonance imaging–negative epilepsies

Yicong Lin[1,2] | Yu-Hua Dean Fang[3] | Guiyun Wu[4] | Stephen E. Jones[5] |

Richard A. Prayson[6] | Ahsan N. V. Moosa[2] | Margit Overmyer[7] | James Bena[8] |

Mykol Larvie[4,5] | William Bingaman[9] | Jorge A. Gonzalez-Martinez[9] | Imad M. Najm[2] |

Andreas V. Alexopoulos[2] | Z. Irene Wang[2]

[1]Department of Neurology, Xuanwu Hospital, Capital Medical University, Beijing, China

[2]Epilepsy Center, Cleveland Clinic, Cleveland, OH, USA

[3]Department of Biomedical Engineering, National Cheng Kung University, Tainan, Taiwan

[4]Department of Nuclear Medicine, Cleveland Clinic, Cleveland, OH, USA

[5]Imaging Institute, Cleveland Clinic, Cleveland, OH, USA

[6]Department of Pathology, Cleveland Clinic, Cleveland, OH, USA

[7]Department of Pediatric Neurology, Helsinki University Hospital, Helsinki, Finland

[8]Department of Quantitative Health Sciences, Cleveland Clinic, Cleveland, OH, USA

[9]Department of Neurosurgery, Cleveland Clinic, Cleveland, OH, USA

Correspondence
Z. Irene Wang, Cleveland Clinic Epilepsy Center, Cleveland, OH, USA.
Email: wangi2@ccf.org

Summary

Objective: Detection of focal cortical dysplasia (FCD) is of paramount importance in epilepsy presurgical evaluation. Our study aims at utilizing quantitative positron emission tomography (QPET) analysis to complement magnetic resonance imaging (MRI) postprocessing by a morphometric analysis program (MAP) to facilitate automated identification of subtle FCD.

Methods: We retrospectively included a consecutive cohort of surgical patients who had a negative preoperative MRI by radiology report. MAP was performed on T1-weighted volumetric sequence and QPET was performed on PET/computed tomographic data, both with comparison to scanner-specific normal databases. Concordance between MAP and QPET was assessed at a lobar level, and the significance of concordant QPET-MAP$^+$ abnormalities was confirmed by postresective seizure outcome and histopathology. QPET thresholds of standard deviations (SDs) of -1, -2, -3, and -4 were evaluated to identify the optimal threshold for QPET-MAP analysis.

Results: A total of 104 patients were included. When QPET thresholds of SD = -1, -2, and -3 were used, complete resection of the QPET-MAP$^+$ region was significantly associated with seizure-free outcome when compared with the partial resection group ($P = 0.023$, $P < 0.001$, $P = 0.006$) or the no resection group ($P = 0.002$, $P < 0.001$, $P = 0.001$). The SD threshold of -2 showed the best combination of positive rate (55%), sensitivity (0.68), specificity (0.88), positive predictive value (0.88), and negative predictive value (0.69). Surgical pathology of the resected QPET-MAP$^+$ areas revealed mainly FCD type I. Multiple QPET-MAP$^+$ regions were present in 12% of the patients at SD = -2.

Significance: Our study demonstrates a practical and effective approach to combine quantitative analyses of functional (QPET) and structural (MAP) imaging data to improve identification of subtle epileptic abnormalities. This approach can

---

Yicong Lin and Yu-Hua Dean Fang contributed equally to this study.

be readily adopted by epilepsy centers to improve postresective seizure outcomes for patients without apparent lesions on MRI.

KEYWORDS
focal cortical dysplasia, MRI postprocessing, MRI-negative epilepsy, presurgical evaluation, quantitative positron emission tomography

1 | INTRODUCTION

In the presurgical evaluation of magnetic resonance imaging (MRI)-negative ("nonlesional") pharmacoresistant focal epilepsy patients, identifying a previously undetected subtle abnormality often helps refocus the surgical hypothesis. Intracranial recordings can sometimes be omitted when the location of the subtle abnormality has good congruence with other noninvasive data. It was shown that many of these previously undetected subtle abnormalities are focal cortical dysplasia (FCD)[1] and can easily be missed during routine visual assessment of MRI because of their small size and subtle morphological characteristics.[2] As such, many MRI postprocessing techniques have been investigated to improve FCD detection.[3-8] A number of studies including our own have shown the usefulness of a morphometric analysis program (MAP), implemented based on algorithms of statistical parametric mapping (SPM) software,[6] to help detect subtle abnormalities in MRI-negative surgical candidates.[6,9–16] One of the shortcomings of the current MAP methodology is that imaging artifacts, registration errors, and normal variants may lead to multiple regions on the output maps with high z scores; some may resemble epileptogenic lesions. To reduce potential false-positive errors, a MAP-guided visual analysis by a dedicated neuroradiologist is needed to decide on the significance of the findings. In this study, we aimed to incorporate information from another noninvasive modality, interictal ^{18}F fluorodeoxyglucose positron emission tomography (PET), to automate the identification of those MAP findings relevant to epilepsy.

As a noninvasive whole-brain imaging modality, PET helps identify and map the metabolic change associated with epilepsy, and therefore should provide complementary functional information to structural MRI postprocessing techniques. The identification of focal PET abnormalities has been shown to help formulate preoperative clinical hypotheses, positively impact intracranial electrode implantation plans, and increase the likelihood of successful surgical intervention.[17-19] Computational tools can help provide objective data and may increase the diagnostic yield of PET, especially in visually "normal" PET scans.[20-24]

In this study, we utilized quantitative processing of PET (QPET) in combination with MAP to automatically and objectively identify epileptogenic abnormalities in a cohort of MRI-negative epilepsy patients. We hypothesized that concordant regions coidentified by MAP and QPET would be epileptogenic, and the resection of these regions would positively associate with more favorable postresective seizure outcomes.

Key Points

- We propose a multimodal approach to combine quantitative analyses of PET and MRI data to improve identification of subtle epileptic abnormalities
- We tested the efficacy of this approach in 104 consecutive patients with a negative preoperative MRI by official radiology report
- Complete resection of the QPET-MAP$^+$ region was significantly associated with seizure-free outcome at QPET SD thresholds of −1, −2, and −3
- The QPET SD threshold of −2 showed the best combination of positive rate, sensitivity, specificity, positive predictive value, and negative predictive value
- Surgical pathology of the resected QPET-MAP$^+$ areas revealed mainly FCD type I

2 | MATERIALS AND METHODS

2.1 | Design and rationale

This retrospective study was approved by the Cleveland Clinic Institutional Review Board. In all patients, the strategies for intracranial electroencephalographic (EEG) implantation and surgical resection were discussed at a patient management conference. Recommendations were made based on available multimodality data that included MRI, seizure semiology, video-electroencephalography, PET, subtraction ictal single photon emission computed tomography (CT) coregistered to MRI, and magnetoencephalography (MEG). The results of QPET-MAP analyses were not used to inform diagnostic and treatment recommendations.

2.2 | Patient selection

We identified patients by reviewing the epilepsy surgical database over a 6-year period (2009-2015). Patients were included if they had (1) a preoperative 1.5-T or 3-T MRI with T1-weighted volumetric sequence, (2) MRI initially read as negative on an official neuroradiology report, (3) a preoperative PET scan on Siemens Biograph PET/CT scanner (Siemens Medical Systems, Erlangen, Germany), (4) >12 months of postsurgical follow-up, and (5) a postoperative MRI. Patients were excluded if they had (1) poor MRI or PET quality hindering clinical read (as stated in the clinical report) or (2) poor MRI or PET quality causing significant registration errors in postprocessing procedures.

2.3 | MRI acquisition and postprocessing

Twenty-five patients had 1.5-T MRI, and 79 patients had 3-T MRI. Detailed MRI parameters and normal database information can be found elsewhere.[12] MAP was processed using SPM12 toolbox (Wellcome Department of Cognitive Neurology, London, UK) in MATLAB 2015a (MathWorks, Natick, MA, USA) following previously established methods.[6,10] MAP was performed on T1-weighted volumetric sequences. For each patient in this study, the main computed output was a junction map, which highlighted brain structures deviating from the average normal database; this difference was measured statistically using a z score, which may indicate the presence of subtle gray-white blurring on the MRI.

2.4 | PET acquisition and QPET

The interictal ^{18}F fluorodeoxyglucose PET/CT was acquired on a Siemens Biograph mCT scanner. Acquisition parameters can be found elsewhere.[25] Simultaneous electroencephalography was acquired during the PET study so that ictal events could be monitored. All patients included in this study had interictal PET. Visual PET analysis results were obtained from the original official PET reports used to guide clinical decisions; the reports were issued by a dedicated nuclear medicine physician (G.W.).

QPET analysis was performed using the Syngo.via software (VB10B; Siemens).[26-28] The attenuation-corrected PET images were first fused with CT via rigid registration and then aligned to a scanner-specific normal database using deformable registration. The PET images were subsequently smoothed using a 12-mm full-width half-maximum isotropic Gaussian kernel to reduce the effect of image noise and nonphysiological intensity variance due to reconstruction. Whole-brain intensity was normalized to eliminate global uptake differences between the patient's PET image and the normal database. Separate normal databases were used depending on patient age: a younger normal database with age range 19-44 years (10 females, 28 males) and an older normal database with age range 46-79 years (22 females, 11 males). Statistical analyses were performed on a voxel basis, and the difference in standard deviations (SDs) compared to the normal database was recorded. This was an automated quantification method, and the results did not depend on the user. The final image output included the original PET images, the QPET images (ie, the statistical maps), and the coregistered MRI images on coronal, axial, and sagittal views; all output images were segmented into predefined sublobar regions. The process also generated a detailed list of standardized uptake values and SDs in comparison with the normal database in all the sublobar regions.

2.5 | QPET-MAP review

Analyses and review of MAP and QPET were performed blinded to patients' clinical information. The candidate MAP[+] regions were defined using a z score threshold of 4 on the junction images, consistent with the literature.[12,14,16] The candidate MAP[+] regions in the entire brain were examined. High z score areas caused by signal inhomogeneity due to technical reasons, nonspecific white matter lesions, and motion or pulsation artifacts were not included. The QPET[+] regions were generated using four different thresholds (SD = $-1, -2, -3, -4$) to evaluate the significance of the QPET-MAP findings at each threshold. For each candidate MAP[+] region, if there was sublobar concordance with a suprathreshold QPET[+] region, or if there was a suprathreshold QPET[+] sublobar region within the same lobe (the whole brain was divided into 12 regions: left and right frontal, parietal, temporal, and occipital lobes, as well as cingulum and insula), then the QPET-MAP[+] analysis was considered positive; otherwise, the QPET-MAP[+] analysis was considered negative. All QPET findings were independently confirmed by a dedicated nuclear medicine physician (G.W.) who was blinded to the clinical data and MAP findings. The final QPET-MAP[+] regions were further re-reviewed by a dedicated neuroradiologist (S.E.J.), who made a judgment as to whether the original MRI showed subtle abnormalities in the QPET-MAP[+] regions. Note that the QPET-MAP[+] regions are the MAP[+] regions with QPET concordance (not the QPET[+] regions with MAP concordance).

2.6 | Asymmetry index

For patients with temporal lobe epilepsy with bilateral temporal hypometabolism shown on QPET, we additionally calculated the asymmetry index based on standardized uptake values of the temporal sublobar regions generated by Syngo.via. Asymmetry ratio was defined by (left − right) / [(left + right) / 2] × 100%.[29] An asymmetry ratio $\leq -10\%$ in any temporal sublobar region was used to indicate left-sided temporal hypometabolism, and an asymmetry ratio

≥10% was used to indicate right-sided temporal hypometabolism.

2.7 | Surgical pathology

Available microscopic slides from surgical resections were re-reviewed in all cases by a dedicated neuropathologist (R.A.P.). FCD was classified according to the International League Against Epilepsy classification.[30] Positive pathology was defined as FCD, hippocampal sclerosis (HS), or other (detailed in Results). Negative pathology was defined by gliosis, hamartia, or the absence of any identifiable microscopic/histological abnormalities.

2.8 | Statistical analyses

The postoperative MRI of each patient was coregistered with the preoperative MRI using SPM12, so that complete or incomplete resections of the QPET-MAP$^+$ regions can be determined. The completeness of resection of the QPET-MAP$^+$ regions was determined by whether the finding was included in the resection cavity on the postoperative MRI. If QPET-MAP$^+$ had multiple findings, all the findings would need to be resected for the case to considered to be completely resected. Surgical outcome at 12 months was classified into two groups: completely seizure-free (Engel class Ia) and not seizure-free (Engel class Ib-IV).[31] We used Pearson chi-square test to assess the relationship of parameters and seizure outcomes; Fisher's exact test was used when the cell size was less than five; t tests and Wilcoxon rank-sum tests were used to compare the association of age and epilepsy duration with outcomes. Positive rates of QPET-MAP were calculated at four QPET SD thresholds: −1, −2, −3, and −4. Sensitivity, specificity, positive predictive value, and negative predictive value were also calculated at these four thresholds. Positive rate is defined as the number of QPET-MAP$^+$ cases/number of the entire cohort. True positive is defined as QPET-MAP$^+$ region fully resected and patient became seizure-free, false positive as QPET-MAP$^+$ region fully resected and patient did not become seizure-free, true negative as QPET-MAP$^+$ region not/partially resected and patient did not become seizure-free, and false negative as QPET-MAP$^+$ region not/partially resected and patient became seizure-free. SAS 9.3 software (SAS Institute, Cary, NC, USA) was used for all analyses. Our study work flow is detailed in Figure 1.

3 | RESULTS

3.1 | Patient demographics

A total of 104 patients fulfilled the study selection criteria. Detailed patient demographics and clinical data are given
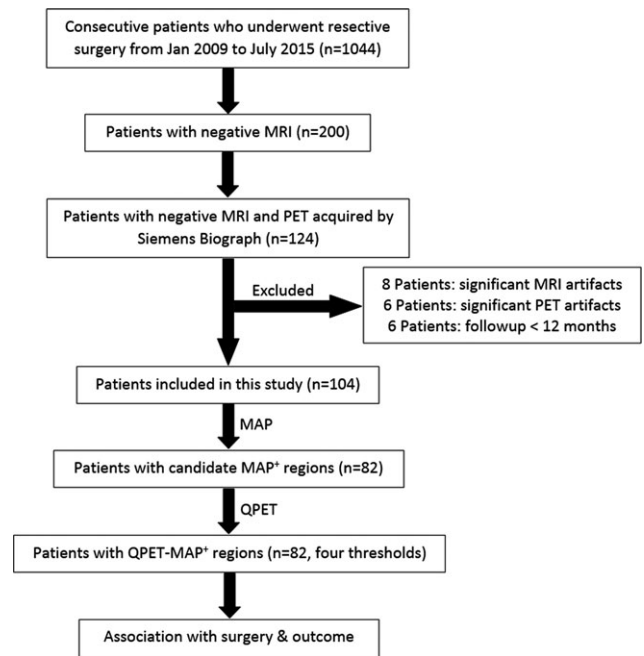

FIGURE 1 Work flow of data collection and analysis. Patients were retrospectively screened according to the inclusion and exclusion criteria. Patients included in the study first underwent morphometric analysis program (MAP) processing. Then, the patients with candidate MAP$^+$ regions underwent quantitative positron emission tomography (QPET) analysis (patients with a MAP-negative finding did not undergo further analysis with QPET). Finally, the QPET-MAP$^+$ regions were compared with the location of surgical resection, and association with seizure outcomes was calculated. MRI, magnetic resonance imaging

in Table 1. Sixty-two of the 104 patients (60%) were seizure-free at 12-month follow-up. Gender, handedness, age, age group (adult or pediatric), epilepsy duration, type of resection (temporal or extratemporal), and type of invasive evaluation were not significantly associated with seizure-free outcome. There was no significant difference in seizure-free outcome between patients who were studied with invasive evaluation and those who were not ($P = 0.39$).

Positive surgical pathology included FCD in 71 (68%), HS in five (5%), FCD associated with HS in two (2%), and other pathology in four (4%, microglial cell proliferation in one and remote infarct in three). In the 71 patients with FCD, FCD IIb was found in six, IIa in six, Ib in 34, and Ic in 25. Seventeen patients (16%) had negative surgical pathology. Five patients (5%) did not have adequate tissue samples for pathological examination. The existence of positive surgical pathology was not associated with seizure-free outcome ($P = 0.86$).

Visual PET analysis on 104 patients revealed 27 lobar localizations, 22 unilateral multilobar findings, 11 bitemporal findings with clear asymmetry, six bitemporal findings without clear asymmetry, 52 bilateral findings (more extensive than bitemporal), and three negative findings. The

TABLE 1 Detailed demographics and clinical data of the 104 patients studied

Factor	Summary	Seizure-free	Not seizure-free	P
Age, y	Mean = 32.3 ± 14.2 (SD), range = 5-65, median = 32	33.8 ± 14.6 (SD), range = 7-65, median = 32	30.2 ± 13.5 (SD), range = 5-64, median = 31.5	0.51[a]
Age group, n (%)				
Age ≥ 18 y	84 (80.8)	52	32	0.33[b]
Age < 18 y	20 (19.2)	10	10	
Epilepsy duration, y	14.3 ± 11.3 (SD), range = 1-53	14.7 ± 11.3 (SD), range = 1-51	13.8 ± 11.3 (SD), range = 1-53	0.36[c]
Gender, n (%)				
Female	50 (48.1)	33	17	0.20[b]
Male	54 (51.9)	29	25	
Handedness, n (%)				
Right	90 (86.5)	53	37	0.70[b]
Left	12 (11.5)	7	5	
Ambidextrous	2 (2)	2	0	
Resection type, n (%)				
Temporal	62 (59.6)	41	21	0.1[b]
Frontal	19 (18.3)	13	6	
Parietal	8 (7.7)	3	5	
Occipital	1 (1.0)	1	0	
Cingulate	2 (1.9)	1	1	
Insular	1 (1.0)	0	1	
Multilobar	11 (10.6)	3	8	
Invasive evaluation type, n (%)				
Subdural grid, with or without depth	18 (24)	14	4	0.1[b]
Stereotactic EEG	55 (73)	29	26	
Both	2 (3)	0	2	
MRI, n (%)				
1.5 T	25 (24)	16	9	0.61[b]
3 T	79 (76)	46	33	

Associations between parameters and seizure outcome at 12 months were tested. Testing of handedness was performed as right versus all others. Testing of resection type was performed as temporal resection versus all others. Testing of invasive evaluation type was performed as subdural grid versus stereotactic EEG. Two patients had subdural grid and stereotactic EEG on two different evaluations.

EEG, electroencephalography; MRI, magnetic resonance imaging; SD, standard deviation.

[a]*t* test.
[b]Pearson chi-square test.
[c]Wilcoxon rank-sum test.

existence of lobar localization by visual PET analysis did not associate with seizure-free outcome (P = 0.39).

3.2 | Candidate MAP+ regions

Candidate MAP+ regions were found in 82 of the 104 patients (79%), including 34 patients with single candidate MAP+ regions and 48 with multiple candidate MAP+ regions (mean = 2.4, median = 2, SD = 0.6, range = 2-4). Twelve (86%) of the 14 patients who had their candidate MAP+ regions completely resected became

seizure-free, 21 (66%) of the 32 patients who had their candidate MAP+ regions partially resected became seizure-free, and 16 (44%) of the 36 patients in whom the candidate MAP+ regions were not included in the resection became seizure-free. Complete resection of the candidate MAP+ regions was not associated with better seizure outcomes when compared to the partial resection group (P = 0.29), but was significantly associated with better seizure outcomes when compared to the no resection group (P = 0.011) and the partial/no resection groups combined (P = 0.037).

3.3 | QPET

QPET analysis on 104 patients revealed 28 lobar localizations, 30 unilateral multilobar findings, four bitemporal findings with clear asymmetry, one bitemporal finding without clear asymmetry, 32 bilateral findings (more extensive than bitemporal), and nine negative findings at the SD threshold of −2. Lobar localization on QPET was not associated with better seizure outcomes ($P = 0.56$). In the 95 patients with positive QPET findings, nine (69%) of the 13 patients who had their QPET regions completely resected became seizure-free (mostly comprised of lobectomies of the hypometabolic temporal lobe); 48 (58%) of the 82 patients in whom the QPET regions were not completely resected became seizure-free. Complete resection of the QPET regions was not associated with seizure-free outcome when compared with the partial/no resection groups combined ($P = 0.55$). In the 62 patients with temporal lobe epilepsy, nine patients had bilateral temporal hypometabolism shown by QPET. Asymmetry index analysis determined the side concordant with surgery in five of these nine patients (56%).

3.4 | QPET-MAP

Combined QPET-MAP analysis was performed on the 82 patients who had candidate MAP$^+$ regions. Table 2 shows the data of QPET-MAP analyses at SD thresholds of −1, −2, −3, and −4. The positive rate of QPET-MAP was 74% (77 of 104) with SD = −1, 55% (57 of 104) with SD = −2, 40% (42 of 104) with SD = −3, and 22% (23 of 104) with SD = −4. At SD = −1, −2, and −3, complete resection of the QPET-MAP$^+$ region was significantly associated with seizure-free outcome when compared with the partial resection group ($P = 0.023$, $P < 0.001$, $P = 0.006$, respectively), the no resection group ($P = 0.002$, $P < 0.001$, $P = 0.001$, respectively), or the partial/no resection groups combined ($P < 0.001$ for all three thresholds). At SD = −4, complete resection of the QPET-MAP$^+$ region was not significantly associated with seizure-free outcome when compared with the partial resection group ($P = 0.119$) or the no resection group ($P = 0.153$), likely due to small sample size. Significance was observed when the partial resection group and the no resection group were combined ($P = 0.04$).

Data for sensitivity and specificity analysis are detailed in Table 3. The threshold of SD = −2 showed the best combination of positive rate (55%), sensitivity (0.68), specificity (0.88), positive predictive value (0.88), and negative predictive value (0.69). At this threshold, re-review of the original MRI scan with a dedicated neuroradiologist confirmed the abnormalities in 88% (50 of 57). Figures 2 and 3 illustrate example patients whose QPET-MAP$^+$

TABLE 2 Correlation between resection of QPET-MAP$^+$ regions and seizure outcomes

Groups, N = 82	Total	Seizure-free, 12 mo	Not seizure-free, 12 mo	P
SD = −1				
Complete resection	23	20	3	<0.001*
Partial resection	23	12	11	0.023
No resection	31	13	18	0.002
Negative	5	4	1	
SD = −2				
Complete resection	25	22	3	<0.001*
Partial resection	11	3	8	<0.001
No resection	21	7	14	<0.001
Negative	25	17	8	
SD = −3				
Complete resection	19	16	3	<0.001*
Partial resection	8	2	6	0.006
No resection	15	4	11	0.001
Negative	40	27	13	
SD = −4				
Complete resection	10	7	3	0.040*
Partial resection	5	1	4	0.119
No resection	8	2	6	0.153
Negative	59	39	20	

P values were generated by Fisher's exact test. The complete resection subgroup was compared with the partial resection and no resection subgroups separately, and also compared with combined subgroups to perform the statistical tests (*P* values indicated by *).

MAP, morphometric analysis program; QPET, quantitative positron emission tomography; SD, standard deviation.

regions were included in the resection and who became seizure-free.

3.5 | Temporal versus extratemporal

We performed subgroup analysis for the 62 patients with temporal lobe epilepsy and the 42 patients with extratemporal lobe epilepsy at threshold of SD = −2. In the extratemporal group, complete resection of QPET-MAP$^+$ regions was positively associated with a seizure-free outcome ($P < 0.01$) when compared with the partial resection group and the no resection group combined. However, in the temporal lobe epilepsy group, the data trended toward but did not reach significance ($P = 0.054$). Lobar localization by visual PET analysis was not associated with better seizure outcomes in either the temporal or the extratemporal group ($P = 0.35$, $P = 0.53$, respectively). Lobar localization by QPET analysis itself (not combined with MAP)

TABLE 3 Positive rate, sensitivity, specificity, PPV, and NPV of QPET-MAP at four thresholds

	SD = −1	SD = −2	SD = −3	SD = −4
Positive rate	74%	55%	40%	22%
Sensitivity (95% CI)	0.44 (0.30-0.60)	0.68 (0.50-0.84)	0.72 (0.50-0.89)	0.70 (0.35-0.93)
Specificity (95% CI)	0.91 (0.75-0.98)	0.88 (0.69-0.97)	0.85 (0.62-0.97)	0.77 (0.46-0.95)
PPV (95% CI)	0.87 (0.66-0.97)	0.88 (0.69-0.97)	0.84 (0.60-0.97)	0.70 (0.35-0.93)
NPV (95% CI)	0.54 (0.40-0.67)	0.69 (0.50-0.84)	0.74 (0.52-0.90)	0.77 (0.46-0.95)

CI, confidence interval; MAP, morphometric analysis program; NPV, negative predictive value; PPV, positive predictive value; QPET, quantitative positron emission tomography; SD, standard deviation.

was not associated with better seizure outcomes in either the temporal or the extratemporal group ($P = 0.21$, $P = 0.43$, respectively).

3.6 | Three tesla versus 1.5 tesla

We further performed subgroup analysis for the 79 patients with 3-T MRI and the 25 patients with 1.5-T MRI, at threshold of SD = −2. In the 3-T group, complete resection of QPET-MAP⁺ regions was positively associated with a seizure-free outcome when compared with the partial resection group ($P = 0.001$), the no resection group ($P = 0.003$), and the partial/no resection groups combined ($P < 0.001$). However, in the 1.5-T group, complete resection of QPET-MAP⁺ regions did not positively associate with a seizure-free outcome when compared with the partial resection group ($P = 0.4$), the no resection group ($P = 0.07$), or combined ($P = 0.1$). Note that there were only 25 patients with 1.5-T MRI, and the small sample size could have contributed to the insignificance.

3.7 | Pathology in patients with QPET-MAP⁺ regions

A total of 36 patients had complete or partial resection of their QPET-MAP⁺ regions at threshold of SD = −2. Positive pathology was found in 32 patients (89%), including FCD in 28, HS in one, microglial cell proliferation in one, and remote infarct in two. In the 28 patients with FCD, FCD IIb was seen in five patients, IIa in five patients, Ib in 12 patients, and Ic in six patients. Notably, all patients who had FCD type IIb (five of five) and type IIa (five of five) in their surgical specimen had the abnormalities confirmed after re-review by the neuroradiologist.

3.8 | Late seizure recurrence

There were 10 patients who became seizure-free at 1-year follow-up without complete resection of the QPET-MAP⁺ regions at the threshold of SD = −2. Five of these 10 patients had seizure recurrence after the first year of

follow-up (two patients in year 2, one in year 3, and two in year 4). Pathology of the five patients with late seizure recurrence showed two gliosis, one Ib, one Ic, and one normal.

3.9 | Multiple QPET-MAP⁺ regions

Twelve patients had multiple QPET-MAP⁺ regions (average = 2.08, median = 2, SD = 0.29, range = 2-3) at the threshold of SD = −2. Eight had the QPET-MAP⁺ regions on the ipsilateral side of the resection (three became seizure-free); in one patient, the abnormality was contralateral to the resection (this patient became seizure-free); in three patients, the abnormalities were bilateral (one became seizure-free).

4 | DISCUSSION

This retrospective study of a large surgical series with postoperative seizure outcomes reveals the usefulness of QPET-MAP analysis in detecting potentially epileptogenic lesions, particularly subtle FCD, in patients considered to have a negative MRI by visual analysis. Results from the automated QPET-MAP analysis were reaffirmed by a neuroradiologist and a nuclear medicine physician. The association found between the resection of the QPET-MAP⁺ regions and good seizure outcome is a strong argument in favor of incorporating a multimodal noninvasive approach into the process of epilepsy presurgical evaluation, particularly in the setting of MRI with no apparent lesion or subtle suspected lesion. The high percentage of patients with FCD upon pathological examination validates the QPET-MAP technique in uncovering potentially epileptic substrates in patients with MRI-negative epilepsy.

4.1 | MAP and QPET used alone and in combination

The most important finding from this study is that the combined MAP and QPET approach has a better yield than
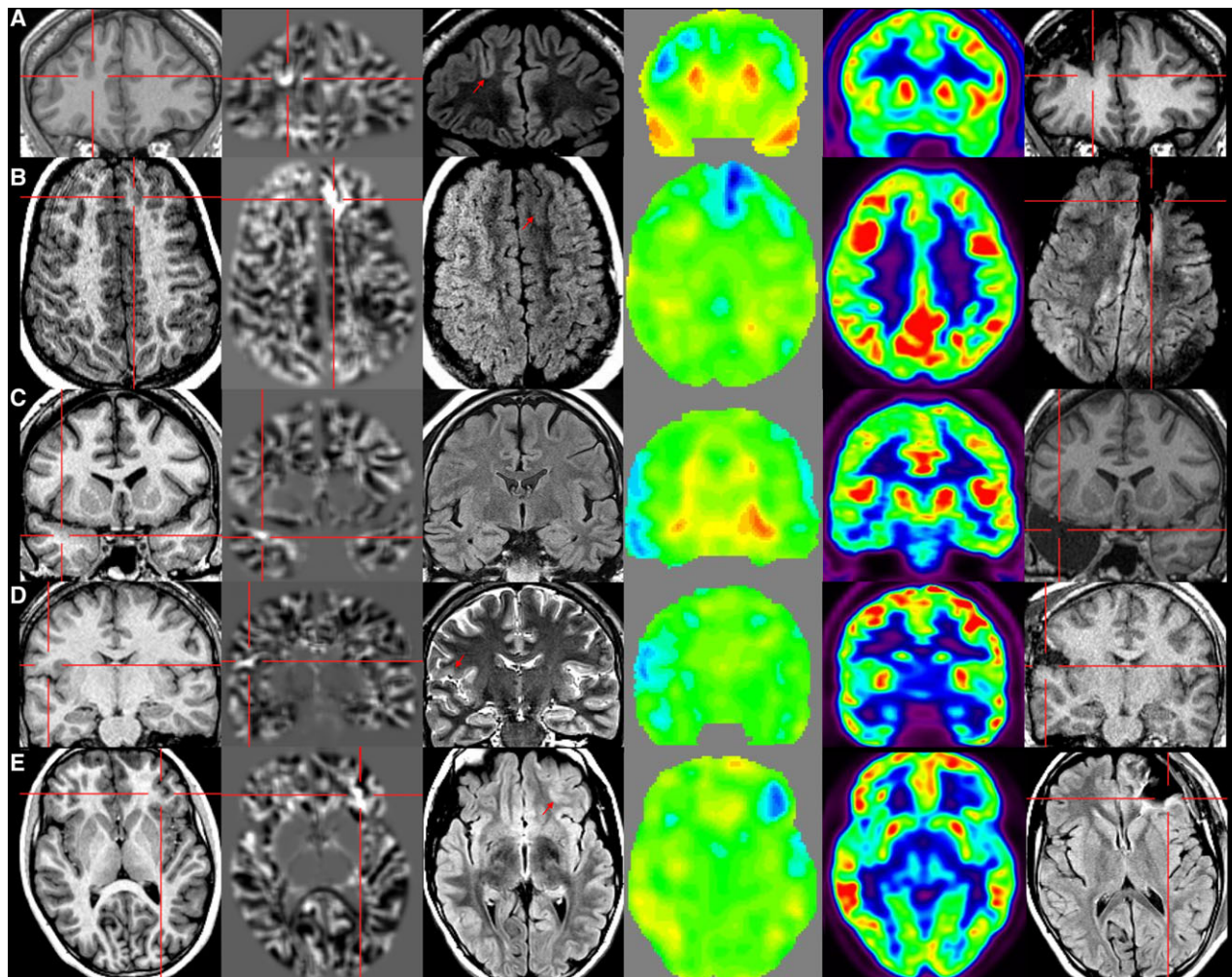
FIGURE 2 Examples of five patients who had a single quantitative positron emission tomography (QPET)-morphometric analysis program (MAP)$^+$ region that was completely included in the surgical resection. In Figures 2 and 3, an SD of -2 was used as the QPET threshold, and the QPET-MAP$^+$ abnormalities were all confirmed by the neuroradiologist re-review. The crosshairs indicate the location of the MAP$^+$ candidate. First column: T1-weighted magnetization prepared rapid acquisition with gradient echo images used during presurgical evaluation. Second column: gray-white matter junction z score file, as the output of MAP processing of the T1-weighted image shown in the first column. Third column: T2-weighted fluid-attenuated inversion recovery or T2-weighted turbo spin echo images, chosen to best depict the MAP$^+$ candidate. Arrows indicate that there were accompanying T2-weighted changes in the MAP$^+$ candidate, and the absence of an arrow indicates that there were no corresponding T2 changes. Fourth column: QPET images as the output of statistic quantitative analysis of the original fluorodeoxyglucose (FDG)-PET image shown in the fifth column. The blue region indicates the hypometabolism, which is consistent with the MAP$^+$ candidate in a lobar range. Fifth column: the original attenuation-corrected FDG-PET images used during presurgical evaluation. Sixth column: postsurgical magnetic resonance imaging indicating site and extent of resection. A, B, QPET-MAP$^+$ region in the frontal lobe; C, QPET-MAP$^+$ region in the temporal lobe; D, E, QPET-MAP$^+$ region in the frontal operculum. All five cases demonstrate complete resection of the QPET-MAP$^+$ region, and all patients remained seizure-free at 12 months. Pathology: A, focal cortical dysplasia (FCD) type IIa; B, C, FCD type Ic; D, E, FCD type IIb. In C, the image in the third column is the best available due to suboptimal slice selection

either QPET or MAP used alone. When MAP is used alone, complete resection of candidate MAP$^+$ regions was significantly associated with seizure-free outcomes when compared with the partial and no resection groups combined ($P = 0.037$); however, most of the significance came from the 34 patients who had a single candidate MAP$^+$ region. When faced with multiple candidate MAP$^+$ regions, distinguishing the true-positive finding from the false-positive findings is a paramount task. In previous studies, a

necessary final step of the MAP methodology is a focused re-review of the MRI by a neuroradiologist using T1, T2, and fluid-attenuated inversion recovery data, to assess for the presence or absence of a subtle but visually identifiable structural change concordant with the MAP-detected region.[6,11,13] This final step is crucial, as suprathreshold regions on the junction output of MAP (or any postprocessing technique) can be caused by imaging artifacts, registration errors, or normal variants, and can resemble a
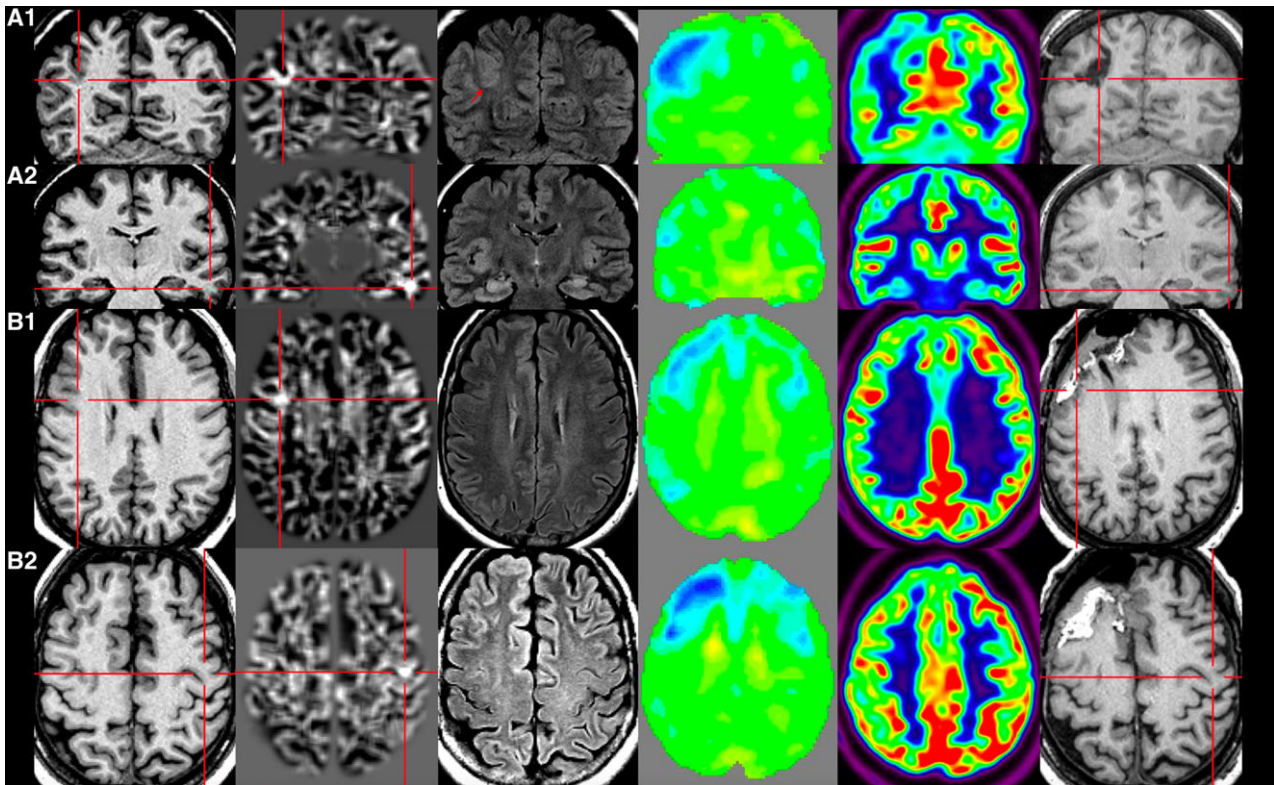
FIGURE 3 Examples of two patients who had multiple candidate morphometric analysis program (MAP)$^+$ regions and quantitative positron emission tomography (QPET) helped distinguish the regions that were relevant to the epilepsy. A, Two candidate MAP$^+$ regions; the one in the right parietal region was QPET-MAP$^+$ and resected (A1), and the other one in the left temporal region was discordant with QPET (therefore QPET-MAP$^-$) and unresected (A2). B, Two candidate MAP$^+$ regions; the one in the right frontal region was QPET-MAP$^+$ and resected (B1), and the other one in the left frontal region was discordant with QPET and unresected (B2). Both cases demonstrate complete resection of the QPET-MAP$^+$ region, and both patients remained seizure-free at 12 months. Pathology: A-1, focal cortical dysplasia (FCD) type IIb; B1, FCD type Ib

true-positive finding. Differentiation of these "artifacts" from true-positive abnormalities inevitably depends on the skills and experience of those reviewing the data. Errors in visual analysis may occur, and true-positive findings may be rejected, such as subtle lesions with only T1 signal changes, which would appear normal on T2-weighted sequences.[13]

When PET is used alone, lobar localization yielded by visual PET analysis or QPET was not associated with seizure-free outcome. This finding is not surprising, as PET often shows areas of hypometabolism extending beyond the epileptogenic region and hence is best suited for lateralization and lobar localization of the potentially epileptogenic region rather than as a precise determination of surgical margins.[19] There is, however, a small subset of patients whose PET studies showed focal abnormalities, particularly the type II group, as exemplified in Figure 1A and 1E.

When used together, the resection of QPET-MAP$^+$ abnormalities was significantly associated with seizure-free outcomes ($P < 0.001$). This is likely due to two factors. First, in the face of multiple candidate MAP$^+$ regions, the epileptogenic subtle abnormalities were kept because of

their lobar concordance with QPET, thus excluding those candidate MAP$^+$ regions that were likely caused by imaging artifacts, registration errors, or nonepileptic variants. Second, the broader localization of QPET is complemented by the more precise localization of potential structural abnormalities identified by MAP. Yield of the combined approach is even higher than the one described in our previous reports using MAP guided by expert neuroradiologist review (56%),[13] suggesting that a combined QPET-MAP approach may be a more sensitive method for the identification of subtle epileptogenic lesions.

4.2 | QPET-MAP findings and surgery

The successful strategy of combining data from multiple noninvasive modalities (structural, electrophysiological, and functional) has been previously reported. In a recent study by Mendes Coelho et al,[26] 39 patients with pharmacoresistant epilepsy and likely FCD were included; a similar approach of examining concordance between QPET and MRI was adopted, and the authors showed that QPET had critical value for patients in the extratemporal group and especially those with subtle MRI findings. Combination of

MRI and PET postprocessing was adopted in a surface-based framework assisted by machine learning in a very recent study that included 28 patients with histopathologically proven FCD.[32] The authors showed that the classifier using combined features from MRI and PET outperformed both quantitative MRI by itself and multimodal visual analysis. In a previous study from our group, we showed that MAP[+] regions with concordant MEG findings were more likely to be epileptogenic in a cohort of 25 MRI-negative patients.[12] Widjaja et al[33] examined PET and MEG in 26 patients with nonlesional MRI and showed that the combination of PET and MEG increased specificity and positive predictive value. Perissinotti et al[34] studied 54 children (26 MRI-negative) and reported that combination of PET and single photon emission CT had localizing results in as high as 76% of the cases. Despite different patient populations and study approaches, these published studies along with our current results suggest that correlating findings from multiple functional and neurophysiological methods improves the identification of epileptogenic pathologies.

4.3 | Temporal lobe versus extratemporal lobe epilepsies

Consistent with the previous literature,[26] our data suggest that QPET-MAP performs better in the extratemporal group than the temporal group. This is probably due to the high proportion of QPET-MAP–negative cases in the temporal group (55%) as compared to the extratemporal group (31%). Note that because of the small number of cases with HS (2%) in surgical pathology, our findings are likely to be more pertinent in those patients with nonlesional neocortical temporal lobe epilepsies,[35,36] rather than patients with classical mesial temporal lobe epilepsies, who are more likely to be MRI-positive. Interestingly, lobar localization of PET hypometabolism by visual analysis or QPET analysis itself (not combined with MAP) did not carry any significant association with seizure-free outcome, further demonstrating challenges presented in this MRI-negative cohort.

4.4 | Asymmetry index analysis in temporal cases

Bilateral temporal hypometabolism can exist in about 10% of patients with medically intractable temporal lobe epilepsy.[37,38] Although these findings may suggest bitemporal independent epileptogenicity, the presence of unilateral mesial temporal epileptic focus with bilateral HS cannot be excluded.[20,39] The asymmetry index analysis used in this study helped lateralize the epilepsy side correctly in 56% (five of nine) of the patients with bilateral temporal hypometabolism. This is consistent with other studies showing

additional lateralization help from asymmetry index analysis,[29] or combination of asymmetry index and extent analysis.[24]

4.5 | Clinical relevance

It is beneficial to ponder the clinical relevance of our findings in the context of preoperative localization and outcome prediction. MAP is considered one of the most well-studied and successful voxel-based techniques for FCD detection[40] and has already been set up in more than 30 centers around the world. QPET can be included as part of the work flow on any Siemens PET/CT scanner. It is foreseeable that combined MAP and QPET analysis results can be provided for consideration (as another non-invasive tool) at multimodal patient management discussions. This process will be especially relevant to those patients with initially negative MRI by visual analysis. If the detected QPET-MAP[+] abnormality is consistent with other electroclinical data, is reaffirmed by the neuroradiologist, and is in a location that is completely resectable, seizure outcome is likely favorable. However, if the reaffirmed finding is in a location that overlaps with eloquent areas and will likely not be completely resected (unless a deficit is acceptable), seizure outcome is likely unfavorable. This information can be useful for discussion with the patient and family. QPET-MAP should be used as a localization test rather than a screening test, because the absence of QPET-MAP[+] abnormality does not preclude the chance of patients becoming seizure-free, as evidenced by our data.

4.6 | Limitations

Patients included in our study were assessed over a 6-year period. Over time, the presurgical evaluation process was not necessarily the same at the beginning and end of this 6-year epoch. For example, 1.5-T MRI was used for earlier patients and 3-T MRI was used for more recent patients. This may have contributed to heterogeneity in the surgical cohort.

Twenty-one of the 104 patients were younger than 19 years of age and therefore outside of the age range (19-44 years) of the PET normal control database; all of them had positive QPET findings. This age mismatch may contribute to more false-positive findings, as reported previously.[41]

5 | CONCLUSIONS

We present a practical and effective approach that combines quantitative analyses of functional (QPET) and

structural (MAP) imaging data to facilitate automated and objective identification of subtle epileptogenic abnormalities. The efficacy of this approach is demonstrated in a large cohort of MRI-negative surgical patients with known pathology and postresective seizure outcomes. This study demonstrates the benefit of combining quantitative analyses of functional and structural imaging modalities in identifying epileptogenic lesions, as has been demonstrated for the integration of other modalities, including MRI, electroencephalography, and MEG. Our findings suggest that this approach may be useful in the evaluation of many and perhaps most patients who have no apparent lesions on structural MRI.

ACKNOWLEDGMENT

DISCLOSURE

The authors have no conflicts of interest to report. We confirm that we have read the Journal's position on issues involved in ethical publication and affirm that this report is consistent with those guidelines.

REFERENCES

1. Wang ZI, Alexopoulos AV, Jones SE, et al. The pathology of magnetic-resonance-imaging-negative epilepsy. Mod Pathol. 2013;26:1051–8.

2. Bernasconi A, Bernasconi N, Bernhardt BC, et al. Advances in MRI for 'cryptogenic' epilepsies. Nat Rev Neurol. 2011;7:99–108.

3. Antel SB. Automated detection of focal cortical dysplasia lesions using computational models of their MRI characteristics and texture analysis. Neuroimage. 2003;19:1748–59.

4. Colliot O. Individual voxel-based analysis of gray matter in focal cortical dysplasia. Neuroimage. 2006;29:162–71.

5. Focke NK, Bonelli SB, Yogarajah M, et al. Automated normalized FLAIR imaging in MRI-negative patients with refractory focal epilepsy. Epilepsia. 2009;50:1484–90.

6. Huppertz HJ, Wellmer J, Staack AM, et al. Voxel-based 3D MRI analysis helps to detect subtle forms of subcortical band heterotopia. Epilepsia. 2008;49:772–85.

7. Riney CJ, Chong WK, Clark CA, et al. Voxel based morphometry of FLAIR MRI in children with intractable focal epilepsy: implications for surgical intervention. Eur J Radiol. 2012;81:1299–1305.

8. Hong SJ, Kim H, Schrader D, et al. Automated detection of cortical dysplasia type II in MRI-negative epilepsy. Neurology. 2014;83:48–55.

9. House PM, Lanz M, Holst B, et al. Comparison of morphometric analysis based on T1- and T2-weighted MRI data for visualization of focal cortical dysplasia. Epilepsy Res. 2013;106:403–9.

10. Huppertz HJ, Grimm C, Fauser S, et al. Enhanced visualization of blurred gray-white matter junctions in focal cortical dysplasia by voxel-based 3D MRI analysis. Epilepsy Res. 2005;67:35–50.

11. Wagner J, Weber B, Urbach H, et al. Morphometric MRI analysis improves detection of focal cortical dysplasia type II. Brain. 2011;134:2844–54.

12. Wang ZI, Alexopoulos AV, Jones SE, et al. Linking MRI postprocessing with magnetic source imaging in MRI-negative epilepsy. Ann Neurol. 2014;75:759–70.

13. Wang ZI, Jones SE, Jaisani Z, et al. Voxel-based morphometric magnetic resonance imaging (MRI) postprocessing in MRI-negative epilepsies. Ann Neurol. 2015;77:1060–75.

14. Wang ZI, Ristic AJ, Wong CH, et al. Neuroimaging characteristics of MRI-negative orbitofrontal epilepsy with focus on voxel-based morphometric MRI postprocessing. Epilepsia. 2013;54:2195–203.

15. Wang ZI, Suwanpakdee P, Jones SE, et al. Re-review of MRI with post-processing in nonlesional patients in whom epilepsy surgery has failed. J Neurol. 2016;263:1736–45.

16. Wellmer J, Parpaley Y, von Lehe M, Huppertz HJ. Integrating magnetic resonance imaging postprocessing results into neuronavigation for electrode implantation and resection of subtle focal cortical dysplasia in previously cryptogenic epilepsy. Neurosurgery. 2010;66:187–194; discussion 194-5.

17. Uijl SG, Leijten FS, Arends JB, et al. The added value of [18F]-fluoro-D-deoxyglucose positron emission tomography in screening for temporal lobe epilepsy surgery. Epilepsia. 2007;48:2121–9.

18. Ollenberger GP, Byrne AJ, Berlangieri SU, et al. Assessment of the role of FDG PET in the diagnosis and management of children with refractory epilepsy. Eur J Nucl Med Mol Imaging. 2005;32:1311–6.

19. Kumar A, Chugani HT. The role of radionuclide imaging in epilepsy, part 1: sporadic temporal and extratemporal lobe epilepsy. J Nucl Med. 2013;54:1775–81.

20. Kim MA, Heo K, Choo MK, et al. Relationship between bilateral temporal hypometabolism and EEG findings for mesial temporal lobe epilepsy: analysis of 18F-FDG PET using SPM. Seizure. 2006;15:56–63.

21. Kumar A, Juhasz C, Asano E, et al. Objective detection of epileptic foci by 18F-FDG PET in children undergoing epilepsy surgery. J Nucl Med. 2010;51:1901–7.

22. Van Bogaert P, Massager N, Tugendhaft P, et al. Statistical parametric mapping of regional glucose metabolism in mesial temporal lobe epilepsy. Neuroimage. 2000;12:129–38.

23. Mayoral M, Marti-Fuster B, Carreno M, et al. Seizure-onset zone localization by statistical parametric mapping in visually normal (18) F-FDG PET studies. Epilepsia. 2016;57:1236–44.

24. Soma T, Momose T, Takahashi M, et al. Usefulness of extent analysis for statistical parametric mapping with asymmetry index using inter-ictal FGD-PET in mesial temporal lobe epilepsy. Ann Nucl Med. 2012;26:319–26.

25. Talanow R, Ruggieri P, Alexopoulos A, et al. PET manifestation in different types of pathology in epilepsy. Clin Nucl Med. 2009;34:670–4.

26. Mendes Coelho VC, Morita ME, Amorim BJ, et al. Automated online quantification method for 18F-FDG positron emission tomography/CT improves detection of the epileptogenic zone in

patients with pharmacoresistant epilepsy. Front Neurol. 2017;8:453.

27. Jena A, Taneja S, Goel R, et al. Reliability of semiquantitative (1)(8)F-FDG PET parameters derived from simultaneous brain PET/MRI: a feasibility study. Eur J Radiol. 2014;83:1269–74.

28. Timerman D, Thum JA, Larvie M. Quantitative analysis of metabolic abnormality associated with brain developmental venous anomalies. Cureus. 2016;8:e799.

29. Kim YK, Lee DS, Lee SK, et al. Differential features of metabolic abnormalities between medial and lateral temporal lobe epilepsy: quantitative analysis of (18)F-FDG PET using SPM. J Nucl Med. 2003;44:1006–12.

30. Blumcke I, Thom M, Aronica E, et al. The clinicopathologic spectrum of focal cortical dysplasias: a consensus classification proposed by an ad hoc Task Force of the ILAE Diagnostic Methods Commission. Epilepsia. 2011;52:158–74.

31. Engel JJ, Van Ness NP, Rasmussen TB, et al. Outcome with respect to epileptic seizures. In: Engel JJ, ed. *Surgical Treatment of the Epilepsies.* New York, NY: Raven Press; 1993:609-21.

32. Tan Y-L, Kim H, Lee S, et al. Quantitative surface analysis of combined MRI and PET enhances detection of focal cortical dysplasias. Neuroimage. 2018;166:10–8.

33. Widjaja E, Shammas A, Vali R, et al. FDG-PET and magnetoencephalography in presurgical workup of children with localization-related nonlesional epilepsy. Epilepsia. 2013;54:691–9.

34. Perissinotti A, Setoain X, Aparicio J, et al. Clinical role of subtraction ictal SPECT coregistered to MR imaging and (18)F-FDG PET in pediatric epilepsy. J Nucl Med. 2014;55:1099–105.

35. Carne RP, Cook MJ, MacGregor LR, et al. "Magnetic resonance imaging negative positron emission tomography positive" temporal lobe epilepsy: FDG-PET pattern differs from mesial temporal lobe epilepsy. Mol Imaging Biol. 2007;9:32–42.

36. Carne RP, O'Brien TJ, Kilpatrick CJ, et al. MRI-negative PET-positive temporal lobe epilepsy: a distinct surgically remediable syndrome. Brain. 2004;127:2276–85.

37. Blum DE, Ehsan T, Dungan D, et al. Bilateral temporal hypometabolism in epilepsy. Epilepsia. 1998;39:651–9.

38. Koutroumanidis M, Hennessy MJ, Seed PT, et al. Significance of interictal bilateral temporal hypometabolism in temporal lobe epilepsy. Neurology. 2000;54:1811–21.

39. Thom M, Martinian L, Catarino C, et al. Bilateral reorganization of the dentate gyrus in hippocampal sclerosis: a postmortem study. Neurology. 2009;73:1033–40.

40. Kini LG, Gee JC, Litt B. Computational analysis in epilepsy neuroimaging: a survey of features and methods. Neuroimage Clin. 2016;11:515–29.

41. Archambaud F, Bouilleret V, Hertz-Pannier L, et al. Optimizing statistical parametric mapping analysis of 18F-FDG PET in children. EJNMMI Res. 2013;3:2.